Fractals, Vol. 24, No. 3 (2016) 1650035 (12 pages)

DOI: 10.1142/S0218348X16500353

World Scientific
www.worldscientific.com

ANALYSIS OF SPONTANEOUS IMBIBITION IN FRACTAL TREE-LIKE NETWORK SYSTEM

CAOXIONG LI,*,† YINGHAO SHEN,*,‡
HONGKUI GE,* SHUAI SU* and ZHIHUI YANG*
*Unconventional Natural Gas Institute
China University of Petroleum, Beijing 102249, P. R. China
†Institute of Mechanics, Chinese Academy of Sciences
Beijing, 100190, P. R. China
‡shenyinghao@126.com

Received October 9, 2015
Accepted April 6, 2016
Published August 10, 2016

Abstract

Spontaneous imbibition in porous media is common in nature, imbibition potential is very important for understanding the imbibition ability, or the ability to keep high imbibition rate for a long time. Structure parameters have influence on imbibition potential. This work investigates the process of spontaneous imbibition of liquid into a fractal tree-like network, taking fractal structure parameters into consideration. The analytical expression for dimensionless imbibition rate with this fractal tree-like network is derived. The influence of structure parameters on imbibition potential is discussed. It is found that optimal diameter ratio β is important for networks to have imbibition potential. Moreover, with liquid imbibed in more sub-branches, some structures of parameter combinations will show the characteristic of imbibition potential gradually. Finally, a parameter plane is made to visualize the percentage of good parameter in all possible combinations and to evaluate the imbibition potential of a specific network system more directly. It is also helpful to design and to optimize a fractal network with good imbibition potential.

Keywords: Porous Media; Imbibition; Fractal; Tree-Like Network.

‡Corresponding author.

1. INTRODUCTION

The spontaneous imbibition in dendritic structures of natural networks is a common phenomenon in nature.[1–3] In early studies, imbibition was investigated in single capillary or a collection of parallel tubes. Imbibition in vertical tube was first introduced by Lucas[4] and Washburn[5] in 1921, they derived an analytical relationship between imbibition distance and imbibition time, called Lucas–Washburn (LW) equation. In the following years, Martic *et al.*[6] pointed out that the contact angle in LW equation should be used as a dynamic contact angle. Cupelli *et al.*[7] pointed out that the inertia of liquid should be taken into account. Fries and Dreyer[8] researched analytic solution of capillary rise in inclined tube. Kim and Whitesides[9] researched capillary rise in noncircular capillaries. Recently, Cai *et al.* studied the effect of tortuosity on capillary rise[10] and introduced fractal theory to modify the LW equation[11] as well as developed a more generalized model for spontaneous imbibition based on Hagen–Poiseuille flow in tortuous capillaries with variably shaped apertures.[12] Yun *et al.*[13] investigated flow rate for power-law fluids in torturous capillary tube by fractal geometry.

Tree-like network model is a tube system with fractal characteristic. It has been used to describe river basins, reservoirs, vein in leaves, economic systems, porous nanofibers, porous media,[14–16] etc. Many natural porous media are fractal, shown by numerous experimental studies. Katz and Thompson[17] might give the first experimental evidence for the fractal features of sandstone samples across three to four orders of magnitude. Studies in the following decades have enhanced this conclusion.[17,18–20] Fractal tree-like network is a proper simplification for porous media. In this network, the diameter and length of the tubes in each branch are developed by fractal law and their ratio between neighboring level is deterministic, which indicates its self-similar properties. The flow and transport phenomenon in this fractal tree-like network have been studied for a long time. Xu *et al.*[21–23] have studied the heat conduction and permeability of this network system, and gave the analysis expression of effective permeability of tree-like network model. Additionally, Xu *et al.*[24–26] enhanced the tree-like network model to a disk-shaped branched network to investigate transport and heat conduction properties. The disk-shaped network model has been well simulated radial flow near wellbore of oil well. Based on the tree-like fractal model above, Wang and Yu discussed low velocity non-Darcy percolation for fractal tree-like network,[27–29] Zheng *et al.* derived the effective permeability and diffusion coefficient of gas in point-to line tree networks.[30,31] Cai[32–34] developed analytical expressions for imbibition process based on fractal characters of porous media and discussed the effect of parameters on imbibition mass and imbibition potential. Pence and Enfield[35,36] computed the pressure and temperature distributions of this fractal-like branching network. The imbibition property of this network system is another interesting area.

Imbibition potential is the probable high imbibition speed for a specific structure of porous media as imbibition time increases. This potential is important to describe imbibition ability. In shale plays, hydraulic fracturing is often used due to the relatively low porosity and permeability, which is related to many parameters. Blocked fracturing liquid in pore structures is critical for gas production.[37–41] For pore structures of shale with high imbibition potential, non-wetting liquid will be absorbed and diffused into gas-saturated porous media with high speed as time goes by, displacing shale gas for a long time and unblocking main flow path of gas. The gas production rate in these formations will not drop abruptly during the production. Optimal pore structures can accelerate the rate of liquid absorption. Recently, Shou *et al.*[42–45] investigated the best structure for the fastest capillary flow in tree-like networks and derived the expression of minimum penetration time in the structure, which verified that optimal pore structures can accelerate rate of liquid absorption.

This work focuses on the imbibition process in fractal tree-like network system. The imbibition potential is represented as the change of imbibition rate in the whole network as imbibition front going into smaller sub-branches. The analytical expression of the imbibition potential is derived and the relationship between the imbibition potential and the structure parameters of the network system is discussed.

2. FRACTAL TREE-LIKE NETWORK SYSTEM

Figure 1 shows the basic structure of fractal tree-like network system, which is generated by

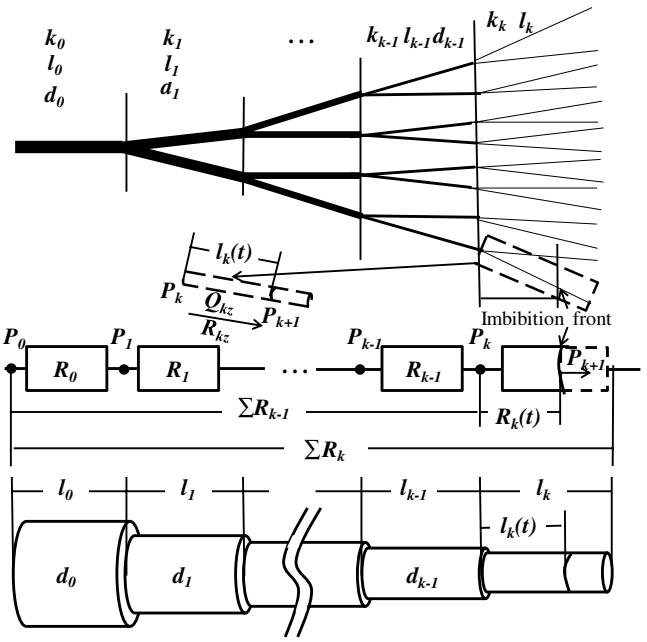

Fig. 1 Schematic of equivalent model of fractal network system.

self-repeating. Each branch of the network is a smooth cylinder. Each cylinder branches into several sub-tubes in the next stage and the diameter and length of tubes in each level decrease gradually. Water is absorbed from the main channel (left tube) and then flow into branches (right) asymptotically. To make some simplifications, we assume the flow as incompressible ideal fluid flowing in cylinder s. Some parameters are needed to describe this model. k represents the branching level (e.g. the main channel is level 0, $k = 0$). A typical branch at some intermediate level k has length l_k and diameter d_k. Supposing the ratio of adjacent level in length and diameter are α and β, these factors are introduced as[22]

$$\alpha = l_{k+1}/l_k, \quad \beta = d_{k+1}/d_k, \tag{1}$$

$$l_k = l_0 a^k, \quad d_k = d_0 \beta^k. \tag{2}$$

By the fractal characteristic of network, α and β remain unchanged. Supposing that every channel is divided into n (branching number) branches at the next level. Level k has N branches, it can be represented as

$$N = n^k. \tag{3}$$

According to the fractal characteristics of the structure,[46] n can be expressed as[22]

$$n = \alpha^{-D_t} = \beta^{-D_d}, \tag{4}$$

where D_l and D_d represent the fractal dimension of throat length and diameter. Fractal dimension varies from 1 to 3. α and D_l can represent the diameter distribution. β and D_d can represent the length distribution.

In natural porous media, the flow channel is not always straight. To take touristy into consideration, Yu[47,48] introduces fractal dimension to represent the tortuosity of capillaries as:

$$l_k = d_k^{1-D_T} L_k^{D_T}, \tag{5}$$

where l_k refers to the length of fluid pathline in kth tube, L_k straight length of tube. D_T refers to the fractal dimension of a tortuous capillary and ranges from 1 to 3. A higher D_T value represents that the capillary is more tortuous and the flow path is also longer.

With the driving of capillary force, liquid imbibes from left to right in this network. The sum of capillary force increases in thinner tubes and with the growing number of tubes. As time goes on, imbibition rate will change due to characteristic of network. Under some circumstances, when the network is well developed, capillary force may be strong enough to overcome the crease of resistance in branch tubes, and then imbibition rate in the network will increase. In this paper, when imbibition rate in first level increases over its average imbibition rate at the beginning of imbibition, this structure is considered to have imbibition potential. The imbibition rate is defined as the liquid volume flowing through any intersecting surface in unit time, or $\overline{Q} = d(V)/dt$, then dimensionless parameter Q^+, defined as the ratio of imbibition rate when liquid flowing in ith level ($\overline{Q_i}$) to initial imbibition rate ($\overline{Q_0}$), $Q^+ = \overline{Q_i}/\overline{Q_0}$, can be regarded as a parameter to represent imbibition potential. When $Q^+ > 1$ at some branching level, the imbibition speed at this level is bigger than the initial imbibition speed, which means this network has the ability to enhance imbibition speed as time goes by.

3. IMBIBITION IN FRACTAL TREE-LIKE NETWORK

Due to the incompressible liquid, the volume flow rate in every level is equal, when imbibition front goes out of the kth level, volume flow rate is

$$Q = \frac{P_{k+1} - P_0}{\sum_{i=0}^{k} R_i}. \tag{6}$$

Capillary pressure in every tube of the kth level is expressed as

$$P_{k+1} = \frac{4\sigma\cos\theta}{d_k}. \tag{7}$$

According to Hagen–Poiseuille equation, the flow rate in every tube of kth level is

$$Q_{ks} = \frac{\pi d_k^4}{128\mu l_k}(P_{k+1} - P_k), \tag{8}$$

$$R_{kz} = \frac{128\mu l_k}{\pi d_k^4}.$$

The total flow rate in tube of kth level is

$$Q_k = n^k Q_{ks} = n^k \frac{\pi d_k^4}{128\mu l_k}(P_{k+1} - P_k). \tag{9}$$

Equation (9) can be mathematically rearranged as

$$Q_k = \frac{P_{k+1} - P_k}{128\mu l_k/(n^k \pi d_k^4)}. \tag{10}$$

Compared to Eq. (6), the total flowing resistance in kth level R_k is

$$R_k = \frac{128\mu l_k}{n^k \pi d_k^4}. \tag{11}$$

When kth channel is filled with liquid, the flowing resistance can be expressed as Eq. (11). From Eqs. (8) and (11), it is shown that flowing resistance in every tube in kth level R_{kz} is n^k times as large as the parallel total resistance in kth level R_k, or $R_{kz} = n^k R_k$.

Imbibition is dynamic. Flowing tube is increasing as imbibition front goes. So the total flow rate in fractal network system can be expressed as:

$$Q_k = \frac{P_{k+1} - P_0}{\sum_{i=0}^{k} R_i} = \frac{P_{k+1} - P_0}{\sum_{i=0}^{k} \frac{128\mu l_i}{n^i \pi d_i^4} + R_k(t)}. \tag{12}$$

Expressing Eq. (12) in other form, from the pressure drop theory, the total pressure drop in system is equal to pressure outlet P_{k+1} minus pressure inlet P_0. It can be expressed as:

$$\begin{aligned} P_{k+1} - P_0 &= \Delta p_k + \Delta p_{k-1} + \cdots + \Delta p_0 \\ &= Q_k R_k(t) + Q_k R_{k-1} + \cdots + Q_k R_0 \\ &= Q_k \left(\sum_{i=0}^{k} R_i\right), \end{aligned}$$

where $R_k(t)$ is total flowing resistance in kth level, when imbibition process is undergoing in kth level. It can be expressed as

$$R_k(t) = \frac{128\mu l_k(t)}{n^k \pi d_k^4} = \frac{128\mu}{n^k \pi d_k^4} \frac{V_k(t)}{\pi d_k^2 n^k/4}, \tag{13}$$

where $V_k(t)$ is the volume of fluid in channel of kth level. According to the definition of flow rate, we have

$$Q_k = dV_k(t)/dt. \tag{14}$$

Integrating Eqs. (12) and (13) to Eq. (14), introducing initial condition as $V_k|_{t=0} = 0$, Eqs. (1) and (2), we have:

$$V_k(t) = \sqrt{\frac{2A}{C}t + \frac{B^2}{C^2}} - \frac{B}{C}, \tag{15}$$

where $A = P_{k+1} - P_0, B = \frac{128\mu l_0}{\pi d_0^4} \frac{1-[\alpha/(n\beta^4)]^k}{1-\alpha/(n\beta^4)}$, $C = \frac{128\mu}{\pi n^k d_0^4 \beta^{4k}} \frac{1}{\pi d_k^2 n^k/4}$.

To simplify this equation, during the period from t_k(the time when fluid flowing into kth channel) to t_{k+1}(the time when fluid flowing out of kth channel), we define average flow rate in kth channel as

$$\overline{Q_k} = \frac{V_k(t_{k+1}) - V_k(t_k)}{t_{k+1} - t_k}. \tag{16}$$

According to mass equation:

$$v_k|_{t=t_k} = 0, \quad v_k|_{t=t_{k+1}} = l_k \pi d_k^2 n^k/4. \tag{17}$$

The gauge pressure of atmosphere this model at the entrance is $P_0 = 0$. Combining Eqs. (15), (1), (2) and (7) with Eq. (16), average flow rate can be expressed as Eq. (18) in kth channel

$$\begin{aligned} \overline{Q_k} = &\frac{4\sigma\cos\theta}{d_0\beta^k} \frac{\pi d_0^4}{128\mu l_0} \\ &\times \left\{\frac{1}{2}\left(\frac{\alpha}{n\beta^4}\right)^k + \frac{1-[\alpha/(n\beta^4)]^k}{1-\alpha/(n\beta^4)}\right\}^{-1}. \end{aligned} \tag{18}$$

To focus on structural factors, fluid effects should be excluded by using dimensionless method. The initial average flow rate is needed. According to Hagen–Poiseuille equation, flow rate in the first level is

$$Q = \frac{P_1 - P_0}{128\mu l/(\pi d_0^4)}, \tag{19}$$

where the relationship between Q and imbibition time t is

$$Q = \frac{dV}{dt} = \frac{\pi d_0^2}{4}\frac{dl}{dt}, \tag{20}$$

where V means fluid volume in capillary. Integrating Eq. (20) to Eq. (19), taking the initial condition

as $l|_{t=0} = 0$, explicit expression is given as

$$l = \sqrt{\frac{P_1 - P_0}{16\mu/d_0^2}t}. \tag{21}$$

When the imbibition front reaches the end capillary of first level, we have

$$l_0 = \sqrt{\frac{P_1 - P_0}{16\mu/d_0^2}t_0}. \tag{22}$$

According to definition, average flow rate in capillary of first level is

$$\overline{Q_0} = \frac{\pi d_0^2}{4}\frac{l_0}{t_0}. \tag{23}$$

Combining Eqs. (22) and (23), the initial average flow rate is

$$\overline{Q_0} = \frac{\pi d_0^4 (P_1 - P_0)}{64\mu l_0}. \tag{24}$$

In the end, combining Eqs. (2), (18) and (24), dimensionless average imbibition flow rate Q^+ in capillary of kth level is

$${Q_k}^+ = \frac{\overline{Q_k}}{\overline{Q_0}} = \frac{1}{\beta^k}\frac{1 - \alpha/(n\beta^4)}{2 - [\alpha/(n\beta^4)]^k[1 + \alpha/(n\beta^4)]}. \tag{25}$$

Or can be expressed with fractal dimension of throat length and diameter distribution as

$$\begin{aligned} {Q_k}^+ &= \frac{\overline{Q_k}}{\overline{Q_0}} \\ &= n^{-k/D_d} \\ &\quad \times \frac{1 - n^{4/D_d - 1 - 1/D_l}}{2 - n^{4k/D_d - k - k/D_l}(1 + n^{4/D_d - 1 - 1/D_l})}. \end{aligned} \tag{26}$$

It is shown that ${Q_k}^+$ is only related to the structure of the model.

4. EXPERIMENT VERIFICATION

To exam the validation of this model, an experiment of imbibition in tree-like model has been made. In this section, tree-like fractal network is carved in plastic board by laser engraving machine. The structure and composition of laser engraving machine is shown in Figs. 2a and 2b. Also, Fig. 2b shows the working state of laser engraving machine. The power of laser gun is 2W. After focusing of laser, this laser gun can generate temperature more than 500° C on the surface of object. Two stepping

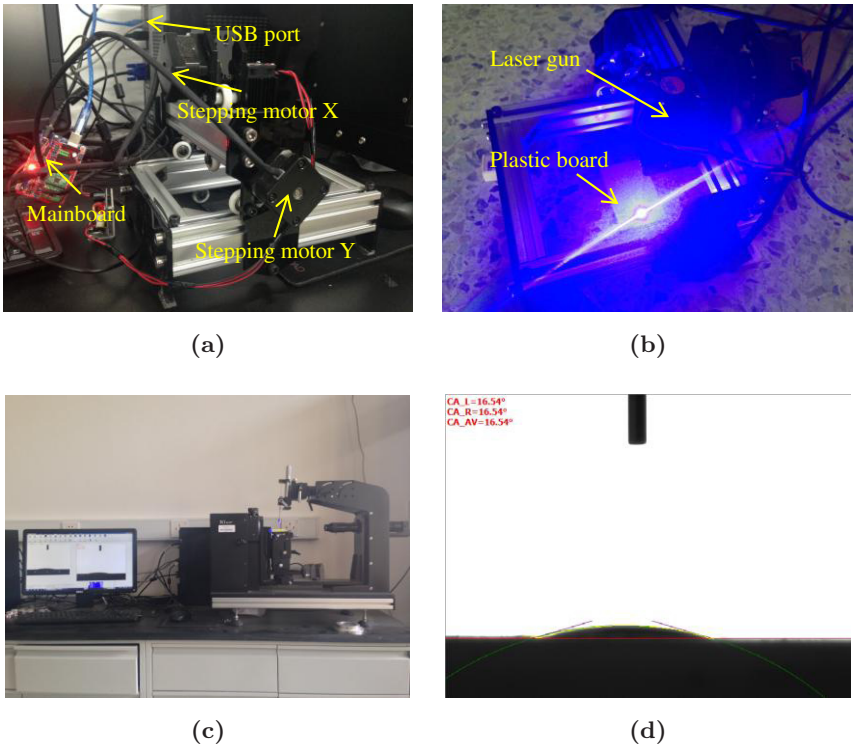

(a) **(b)**

(c) **(d)**

Fig. 2 Laser engraving machine and contact angle meter. **(a)** Basic structure of laser engraving machine, **(b)** working status of laser engraving machine, **(c)** contact angle meter and **(d)** result of contact angle test.

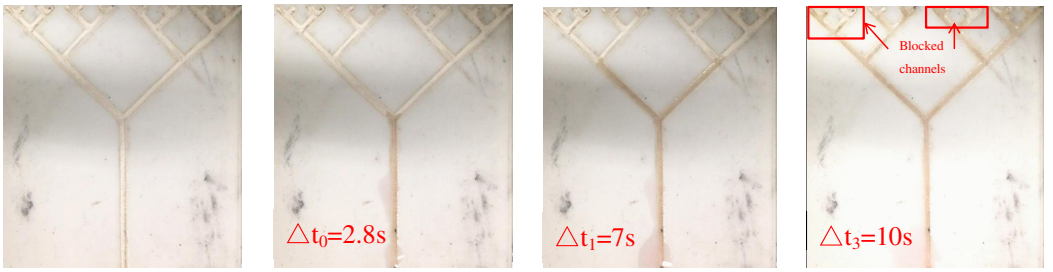

Fig. 3 Kerosene diffusing in tree-like fractal network. **(a)** Empty network, **(b)** the first level branch is filled with kerosene, **(c)** the second level branch is filled with kerosene and **(d)** the network is almost filled with kerosene, by some accident, a small fraction of the last stage is not filled by kerosene. From the video calculation, the time spent in the first level is about 2.8 s, or $\Delta t_0 = 2.8$ s, and so on, $\Delta t_1 = 7$ s, $\Delta t_2 = 9$ s, $\Delta t_3 = 10$ s. However, due to the blocked channels in the last level, t_3 is calculated by average pass-through time without blocked channels.

motors (on direction X and Y) can drive the laser gun move at the same height. The angle-position precision of motors are 0.9a. These motors are controlled by mainboard connecting to computer with USB port. We programmed the movement of laser gun on computer by G code. A plastic board is set under the laser gun. High temperature generated by laser melted and scorched the plastic and curved tree-like fractal network on plastic board. We covered and pasted the curved board with a transparent plastic board to observe the imbibition process in tree-like fractal network. In this work, we generated a tree-like network with parameters as $\alpha = 0.5, \beta = 1, n = 2, k = 4, l_0 = 28.5$ mm and $d_0 = 1$ mm. The imbibition liquid is kerosene. Its viscosity is 0.91 mPas and density is 0.8×10^3 kg/m^3. The contact angle between kerosene and plastic is measured by contact angle meter, shown in Figs. 2c and 2d, the result is 16.54°.

To verify the accuracy of our imbibition equation, we video the process of imbibition and calculate the average time spent in every stage of channel. The environment temperature during imbibition process is 18.6° C. As shown in Fig. 3, the imbibition front can be observed clearly. At every branching point, imbibition front split and flow into two sub-channels. Calculated from the recorded video, the time spent in the first level is about 2.8 s, or $\Delta t_0 = 2.8$ s, and $\Delta t_1 = 7$ s, $\Delta t_2 = 9$ s, $\Delta t_3 = 10$ s. Unfortunately, with the contingency and uncontrollability of experimental environment, a small fraction of channels in the last level are blocked, so Δt_3 is calculated by average pass-through time without blocked channels, which makes Δt_3 not actually very accurate. Anyway, we calculated average flow rate in each level by Eq. (27) and dimensionless flow rate by Eq. (28).

$$\overline{Q_k} = \frac{V_k}{\Delta t_k}, \tag{27}$$

$$Q_k^+ = \frac{\overline{Q_k}}{\overline{Q_0}}. \tag{28}$$

Meanwhile, we compare the experimental data with theoretical data calculated by Eq. (25). The result is shown in Fig. 4. It shows that most of the theoretical data coordinate well with the experimental data from $k = 0$ to 2, which validates our calculation of dimensionless average imbibition flow rate in capillary of kth level, or Eq. (25). Because of the roughness of channel wall and contingency of liquid, it is hard to control fluid in every channel

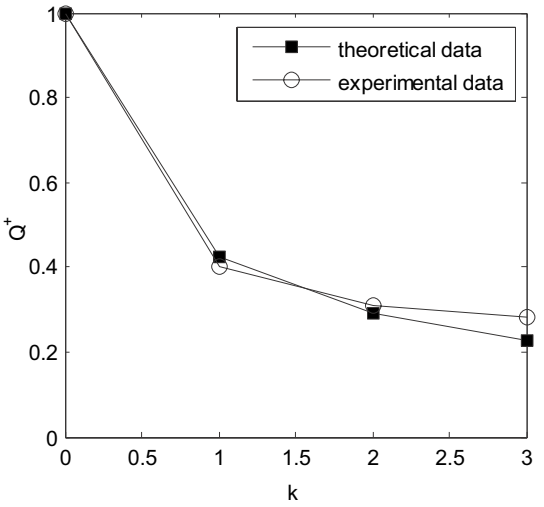

Fig. 4 Validation of tree-like fractal model. Most of the theoretical data well coordinate with experimental data. With some channels blocked in the last level, Q^+ is deviated from theoretical data at $k = 3$.

reach its branching point simultaneously, especially in the last level, the deviation at $k = 3$ is not universal.

5. RESULTS AND DISCUSSIONS

In this section, the influence of the geometrical structures on the dimensionless imbibition rate is discussed. Figure 5 shows the dimensionless imbibition rate ${Q_k}^+$ versus the branching level k with different structure parameters. These parameters have length ratios α, the diameter ratios β and the branching number n. Generally, ${Q_k}^+$ reduces with k at the beginning of imbibition, with the increase of k, ${Q_k}^+$ may increase (Figs. 5a and 5b). That means imbibition rate generally decreases when imbibition front is absorbed in smaller tubes. But when α is small enough or β is big enough, like $\alpha = 0.4$ or $\beta = 0.7$, ${Q_k}^+$ will become bigger as k increases. D_l and D_d are another way to express α and β according to Eq. (4). So the trend in Figs. 5c and 5d are similar to that in Figs. 5a and 5b. When n increases, ${Q_k}^+$ in latter levels increases obviously (Fig. 2e). To sum up, dimensionless imbibition rate generally decreases as imbibition front moves in smaller tubes at first, but when α is small enough, imbibition

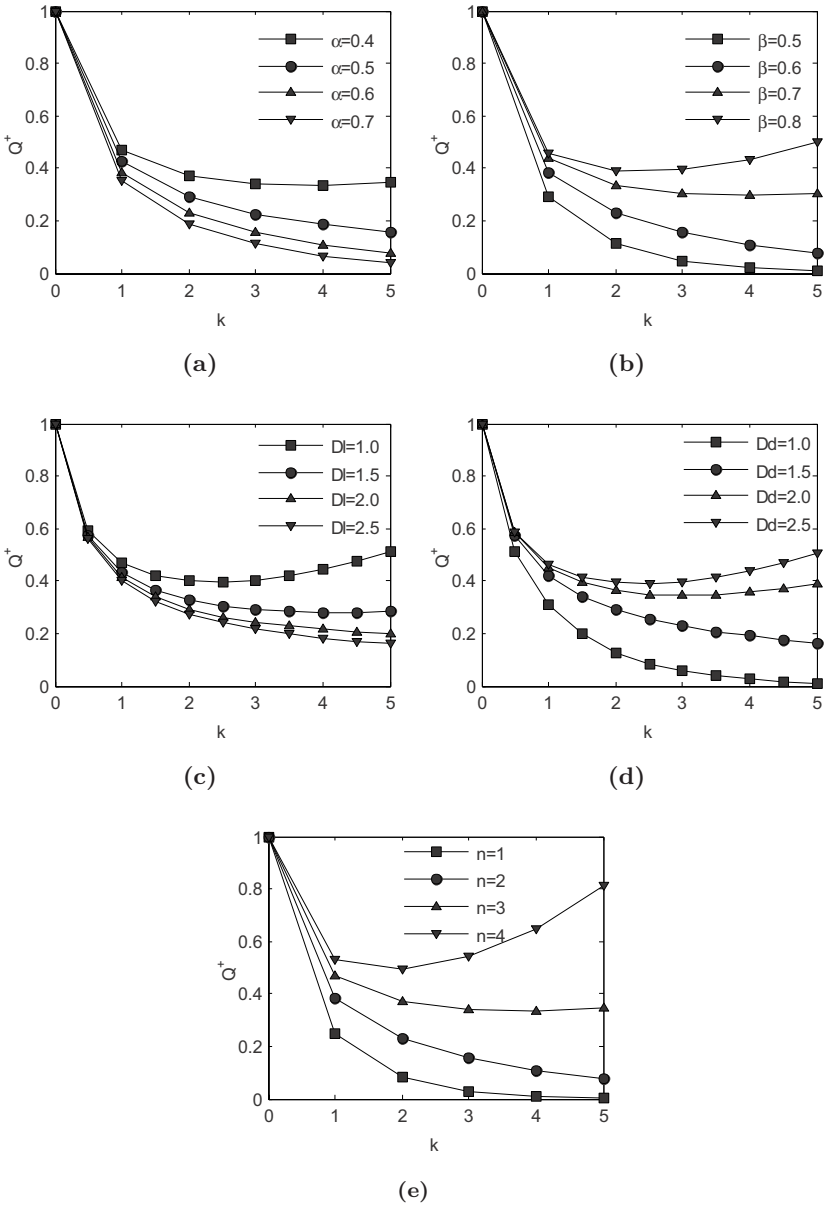

Fig. 5 The curve of dimensionless average imbibition rate versus imbibition branching level. **(a)** $\beta = 0.6\, n = 2$, **(b)** $\alpha = 0.6\, n = 2$, **(c)** $D_d = 2\, n = 2$, **(d)** $D_l = 1.2\, n = 2$ and **(e)** $\alpha = 0.6\, \beta = 0.6$.

front is easier to go to the next level. That means more branches will be filled with water, so $Q_k{}^+$ may increase. Larger n can accelerate this process. If β is not too small, the advantage of increasing branching number will compensate the disadvantage of the decreasing pore size. So smallerand not too small β in pore structure will have good imbibition performance, like Fig. 5e.

Structure parameters have influence on dimensionless imbibition rate within the same branching level ($k = 5$) (Fig. 6). When β is not too small, smaller α and bigger n will obviously increase $Q_k{}^+$ (e.g. $\alpha < 0.4$ and $n > 3$). Otherwise when β is too small (e.g. $\beta < 0.4$), $Q_k{}^+$ remains low no matter how α and n change (Figs. 6a and 6b). This is because pore diameter will be too thin in next level, then resistance will obviously increase, more branches and higher capillary force cannot compensate the energy loss of fluid. There is a set of optimum combination of parameters when β ranges between 0.6 and 1. When $\alpha < 0.2$, β and n have impact on $Q_k{}^+$, if α grows bigger than 0.6, fluid will take long way to enter the next level, which have a negative effect on the imbibition process.

There are two prerequisites for fractural tree-like network having imbibition potential, or having possibility to gain faster imbibition rate in imbibition process. One is that it has good parameter combination of structure, or the coordination of D_l, D_d (or α, β) and n. The other is that branches are well developed, or branching level k is large enough. To investigate the percentage of good parameter in all possible combinations, a parameter plane can be made, which is a flat filled with all possible $Q_k{}^+$ when n and k are stable, with two axes D_l and D_d. Parameter combinations making $Q_k^+ > 1$ are called good parameter combinations (to have imbibition potential), while the parameter combination making biggest $Q_k{}^+$ is called best parameter combination (to have imbibition potential). Moreover, this parameter plane helps not only to evaluate how many combinations are good in all possible combinations but also to evaluate a specific parameter combination by what zone it falls in. When it falls in $Q_k^+ > 1$, the fractural tree-like network having this parameter combination has imbibition potential, otherwise it has not. Additionally, when it comes to optimizing a fractal network, this parameter plane

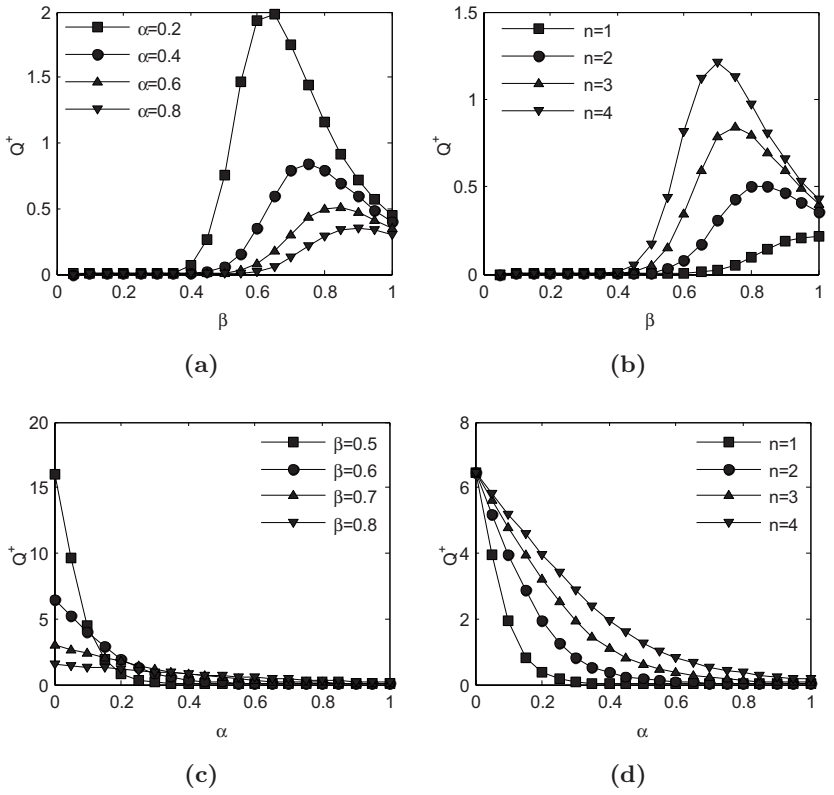

Fig. 6 Impact of structure parameters on dimensionless imbibition rate within the same branching level. **(a)** $k = 5\, n = 2$, **(b)** $k = 5\, \alpha = 0.6$, **(c)** $k = 5\, n = 2$ and **(d)** $k = 5\, \beta = 0.6$.

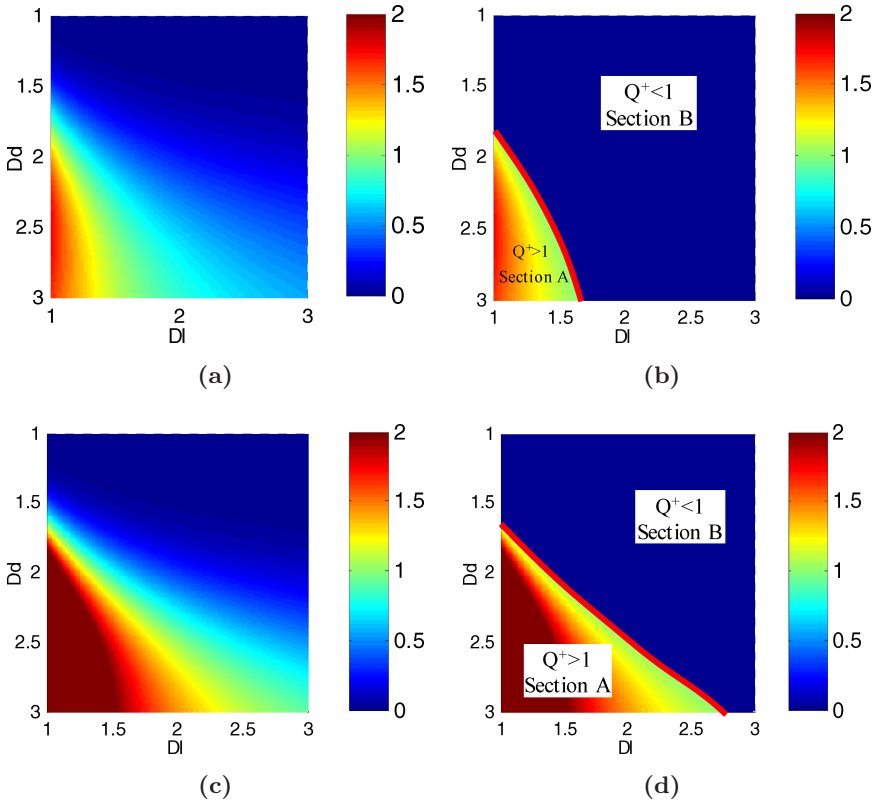

Fig. 7 Parameter plane of different branching numbers at the same branching level. **(a)** $k=5\,n=3$, **(b)** $k=5\,n=3$, **(c)** $k=5\,n=4$ and **(d)** $k=5\,n=4$.

will make this work more efficient because the best parameter combination can be found directly. By fraction theory, Q_k^+ should be under the boundary condition of $1 < D_t < 3, 1 < D_d < 3$.

Figure 7 shows a parameter plane of different branching numbers at the same branching level, Figs. 7b and 7d is the result of deleting $Q_k^+ < 1$ the combinations in Figs. 7a and 7c. It denotes that with branching number n increasing from 3 to 4, parameter combinations to have imbibition potential increases from 11.9% to 30.0%. It is expected because larger branching number can make more branches, which increases the sum of capillary force and makes more combinations become potential.

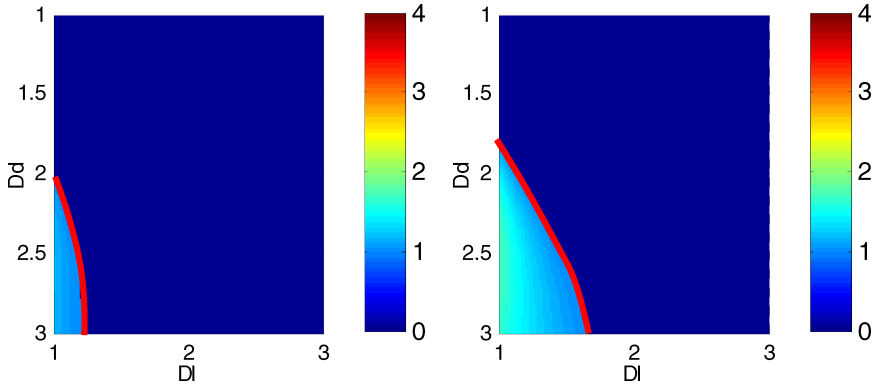

Fig. 8 Parameter plane of different branching levels at the same branching number. **(a)** $k = 4\,n = 3$, **(b)** $k = 5\,n = 3$, **(c)** $k = 6\,n = 3$ and **(d)** $k = 7\,n = 3$.

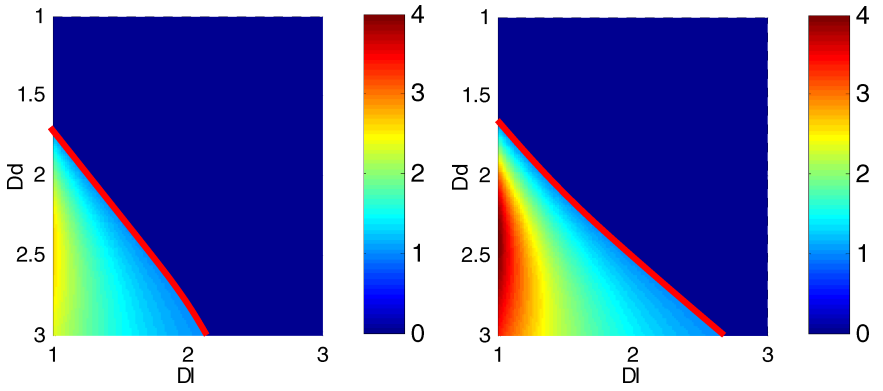

Fig. 8 (*Continued*)

The best parameter combination locates in small D_l and appropriate or not too small D_d, this is consistent with conclusions in Fig. 5.

Figure 8 shows parameter plane of different branching levels at the same branching number. Similarly, the combinations $Q_k^+ < 1$ of are deleted from this figure. It shows that, with the increasing of branching level k, parameter combinations to have imbibition potential increases from 6.24% to 27.56%. That is to say, with liquid imbibe in more sub-branches (or with time increases), some structures will have imbibing potential. In this process, at the zone of best parameter combinations, dimensionless imbibition rate increases sharply.

6. CONCLUSIONS

In this paper, the process of spontaneous imbibition of liquid into a fractal tree-like network is investigated, taking structure parameters into consideration. An analytical expression of dimensionless imbibition rate in this fractal tree-like network is derived, given by Eqs. (25) and (26). It is found that generally speaking, the smaller the length ratio α is, the higher imbibition potential the tree-like network may have. With smaller α, the length of sub-channels will decrease sharply. It makes easier for liquid to flow into sub-channels and spread away, which are positive to imbibition potential. And larger diameter ratio β makes wider sub-channels for liquid, which also makes easier for liquid to flow into sub-channels. Larger branching number n and branching level k can help the network to have imbibition potential because these two parameters can surge the number of sub-channels in spontaneous imbibition process. The imbibition potential of the network will be negligible when β is too small, no matter how α and β change, because small β will lead sub-channels too thin to flow. Thin channels increase the flowing residence, which is negative to imbibition potential. Besides, when $\beta > 0.4$, a slight change of α and n will make a significant influence on imbibition potential. Moreover, with liquid imbibing into more sub-branches, some structures will show positive characteristic to imbibition potential gradually.

Additionally, with the fractal characteristics, α and β can be represented by fractal dimension D_l and D_d, respectively. A parameter plane is made to visualize the percentage of good parameter in all possible combinations and to evaluate the imbibition potential of a specific network system more directly, which is useful. Also, this plane can help the work of designing and optimizing a fractal network with good imbibition potential.

ACKNOWLEDGMENTS

This work was supported by the National 973 Program (Grant No. 2015CB250903), the Major Program of the National Natural Science Foundation of China (Grant Nos. 51490652 and U1562215) and the Science Foundation of China University of Petroleum, Beijing (Grant Nos. YJRC-2013-17 and 2462015YQ1202).

REFERENCES

1. A. Bejan and M. R. Errera, Deterministic tree networks for fluid flow: geometry for minimal flow resistance between a volume and one point, *Fractals* **5**(04) (1997) 685–695.
2. M. S. Singleton, G. Heiss and A. Hübler, Optimization of ramified absorber networks doing desalination, *Phys. Rev. E* **83**(1) (2011) 016308.

3. T. D. Wheeler and A. D. Stroock, The transpiration of water at negative pressures in a synthetic tree, *Nature* **455**(7210) (2008) 208–212.
4. R. Lucas, Rate of capillary ascension of liquids, *Kolloid Z.* **23**(15) (1918) 15–22.
5. E. W. Washburn, The dynamics of capillary flow, *Phys. Rev.* **17**(3) (1921) 273.
6. G. Martic *et al.*, A molecular dynamics simulation of capillary imbibition, *Langmuir* **18**(21) (2002) 7971–7976.
7. C. Cupelli *et al.*, Dynamic capillary wetting studied with dissipative particle dynamics, *New J. Phys.* **10**(4) (2008) 043009.
8. N. Fries and M. Dreyer, An analytic solution of capillary rise restrained by gravity, *J. Colloid Interface Sci.* **320**(1) (2008) 259–263.
9. E. Kim and G. M. Whitesides, Imbibition and flow of wetting liquids in noncircular capillaries, *J. Phys. Chem. B* **101**(6) (1997) 855–863.
10. J. C. Cai, B. M. Yu, M. F. Mei *et al.*, Capillary rise in a single tortuous capillary, *Chin. Phys. Lett.* **27**(5) (2010) 054701.
11. J. C. Cai and B. M. Yu, A discussion of the effect of tortuosity on the capillary imbibition in porous media, *Transp. Porous Media* **89**(2) (2011) 251–263.
12. J. C. Cai, E. Perfect, C. L. Cheng *et al.*, Generalized modeling of spontaneous imbibition based on Hagen–Poiseuille flow in tortuous capillaries with variably shaped apertures, *Langmuir* **30**(18) (2014) 5142–5151.
13. M. J. Yun, B. M. Yu, X. Peng *et al.*, Fractal analysis of power-law fluid in a single capillary, *Chin. Phys. Lett.* **25**(2) (2008) 616.
14. B. Q. Xiao, J. T. Fan, Z. C. Wang *et al.*, Fractal analysis of gas diffusion in porous nanofibers, *Fractals* **23**(1) (2015) 1540011.
15. N. MacDonald, *Trees and Networks in Biological Models* (John Wiley, New York, 1971).
16. F. Cramer, *Chaos and Order*: *The Complex Structure of Living Systems* (VCH, New York, 1993).
17. A. J. Katz and A. H. Thompson, Fractal sandstone pores: Implications for conductivity and pore formation, *Phys. Rev. Lett.* **54** (1985) 1325–1328.
18. M. Sheng, G. S. Li, S. C. Tian *et al.*, A fractal permeability model for shale matrix with multiscale porous structure, *Fractals* (2016) 1650002.
19. G. B. West, J. H. Brown and B. J. Enquist, A general model for the origin of allometric scaling laws in biology, *Science* **276**(5309) (1997) 122–126.
20. C. E. Krohn, Fractal measurements of sandstones, shales, and carbonates, *J. Geophys. Res*: *Solid Earth* **93**(B4) (1988) 3297–3305.
21. P. Xu, A discussion on fractal models for transport physics of porous media, *Fractals* **23**(3) (2015) 1530001.
22. P. Xu *et al.*, Analysis of permeability for the fractal-like tree network by parallel and series models, *Physica A* **369**(2) (2006) 884–894.
23. P. Xu *et al.*, Heat conduction in fractal tree-like branched networks, *Int. J. Heat Mass Transfer* **49**(19) (2006) 3746–3751.
24. P. Xu, B. M. Yu, Y. Feng *et al.*, Permeability of the fractal disk-shaped branched network with tortuosity effect, *Phys. Fluids* **18**(7) (2006) 078103.
25. P. Xu and B. M. Yu, The scaling laws of transport properties for fractal-like tree networks, *J. Appl. Phys.* **100**(10) (2006) 104906.
26. P. Xu, B. M. Yu, S. Qiu *et al.*, An analysis of the radial flow in the heterogeneous porous media based on fractal and constructal tree networks, *Physica A* **387**(26) (2008) 6471–6483.
27. S. F. Wang, B. M. Yu, Q. Zheng *et al.*, A fractal model for the starting pressure gradient for Bingham fluid in porous media embedded with randomly distributed fractal-like tree networks, *Adv. Water Resour.* **34** (2011) 1574–1580.
28. S. F. Wang and B. M. Yu, Study on the effect of capillary pressure on the permeability of porous media embedded with a fractal-like network, *Int. J. Multiphase Flow* **37** (2011) 507–513.
29. S. F. Wang and B. M. Yu, A fractal model for the starting pressure gradient for Bingham fluids in porous media embedded with fractal-like tree networks, *Int. J. Heat Mass Transfer* **54** (2011) 4491–4494.
30. Q. Zheng and B. M. Yu, A fractal permeability model for gas flow through dual-porosity media, *J. Appl. Phys.* **111** (2012) 024316.
31. Q. Zheng, J. Xu, B. Yang and B. M. Yu, Research on the effective gas diffusion coefficient in dry porous media embedded with a fractal-like tree network, *Physica A* **392** (2013) 1557–1566.
32. J. C. Cai, L. Luo, R. Ye, X. F. Zeng *et al.*, Recent advances on fractal modeling of permeability for fibrous porous, *Fractals* **23** (2015) 1540006.
33. J. C. Cai, B. M. Yu, M. Q. Zou *et al.*, Fractal characterization of spontaneous co-current imbibition in porous media, *Energy Fuel* **24**(3) (2010) 1860–1867.
34. J. C. Cai and S. Sun, Fractal analysis of fracture increasing spontaneous imbibition in porous media with gas-saturated, *Int. J. Mod. Phys. C* **24**(08) (2013) 1350056.
35. D. V. Pence, Reduced pumping power and wall temperature in microchannel heat sinks with fractal-like branching channel networks, *Microsc. Therm.* **6**(4) (2003) 319–330.
36. D. V. Pence and K. Enfield, Inherent benefits in microscale fractal-like devices for enhanced transport phenomena, *Des. Nature* **6** (2004) 317–327.
37. B. Yuan, Y. Su and R. G. Moghanloo, A new analytical multi-linear solution for gas flow toward

fractured horizontal well with different fracture intensity, *J. Nat. Gas. Sci. Eng.* **23** (2015) 227–238.
38. B. Yuan, R. G. Moghanloo, E. Shariff *et al.*, Integrated investigation of dynamic drainage volume (DDV) and inflow performance relationship (Transient IPR) to optimize multi-stage fractured horizontal wells in shale oil, *J. Energ. Resour. Tech.* **138**(5) (2016) 052901.
39. R. G. Moghanloo, B. Yuan, N. Ingrahama *et al.*, Applying macroscopic material balance to evaluate dynamic drainage volume and performance prediction of shale oil/gas wells, *J. Nat. Gas Sci. Eng.* **27** (2015) 466–478.
40. B. Yuan, D. A. Wood and W. Yu, Stimulation and hydraulic fracturing technology in natural gas reservoirs: Theory and case study (2012–2015), *J. Nat. Gas Sci. Eng.* **26** (2015) 1414–1421.
41. B. Yuan and D. A. Wood, Production analysis and performance forecasting for natural gas reservoirs: Theory and practice (2011–2015), *J. Nat. Gas Sci. Eng.* **26** (2015) 1433–1438.
42. D. H. Shou and J. T. Fan, The fastest capillary penetration of power-law fluids, *Chem. Eng. Sci.* **137** (2015) 583–589.
43. D. H. Shou and J. T. Fan, Structural optimization of porous media for fast and controlled capillary flows, *Phys. Rev. E* **91**(5) (2015) 053021.
44. D. H. Shou, L. Ye and J. T. Fan, Treelike networks accelerating capillary flow, *Phys. Rev. E* **89**(5) (2014) 053007.
45. D. H. Shou, L. Ye, J. T. Fan *et al.*, Optimal design of porous structures for the fastest liquid absorption, *Langmuir* **30**(1) (2013) 149–155.
46. B. B. Mandelbrot, *The Fractal Geometry of Nature* (W. H. Freeman, San Francisco, 1982).
47. B. M. Yu and P. Cheng, A fractal permeability model for bi-dispersed porous media, *Int. J. Heat Mass Transfer* **45**(14) (2002) 2983–2993.
48. B. M. Yu, J. C. Cai and M. Q. Zou, On the physical properties of apparent two-phase fractal porous media, *Vadose Zone J.* **8**(1) (2009) 177–186.